ROBUST SNAKE CONVERGENCE BASED ON DYNAMIC PROGRAMMING

A.K. Mishra, P. Fieguth, D.A. Clausi.

Vision and Image Processing Research Group, Systems Design Engineering,
University of Waterloo, Waterloo, ON, Canada
{akmishra, pfieguth, dclausi}@engmail.uwaterloo.ca

ABSTRACT

The extraction of contours using deformable models, such as snakes, is a problem of great interest in computer vision, particular in areas of medical imaging and tracking. Snakes have been widely studied and many methods are available. In most cases, the snake converges towards the optimal contour by minimizing a sum of internal (prior) and external (image measurement) energy terms. This approach is elegant, but frequently mis-converges in the presence of noise or complex contours.

To address these limitations, a novel discrete snake is proposed which treats the two energy terms separately. Essentially, the proposed method is a deterministic iterative statistical data fusion approach, in which the visual boundaries of the object are extracted, ignoring any prior, employing a Hidden Markov Model (HMM) and Viterbi search, and then applying importance sampling to the boundary points, on which the shape prior is asserted. The proposed implementation is straightforward and achieves dramatic speed and accuracy improvement compared to other methods.

***Index Terms*—** Snake, Curvature guided importance sampling, HMM, Viterbi Algorithm, Statistical data fusion

1. INTRODUCTION

Locating the exact boundaries of objects has many applications in object tracking [1], content based image and video retrieval systems [2], robotics and biomedical engineering [3]. Energy minimizing splines, such as deformable snakes or active contours, are the key approaches in the computer vision literature for such boundary extraction problems. The principal idea in active contour modeling is to minimize the sum of internal (prior) and external (image-based) energies to obtain an optimum boundary. The internal energy typically asserts a first- or second-order smoothness constraint on the boundary, whereas the external energy applies a “force” on the boundary, creating an attractive force towards areas of high gradient. Since the original development of snake methods [1], many modifications have been attempted to overcome various shortcomings, primarily concentrated on altering the external energy, such as pressure based balloon force [3], distance transformed image gradient [4, 2], and gradient vector flow [5].

Traditional snakes have two problems. First, if the initial position is too far from the object boundary then the snake requires many iterations (and thus a long time) to converge, a particular concern in tracking or real-time problems. Second, standard snake algorithms do not guarantee convergence and tend to be very sensitive to noise and false weak edges. Both of these difficulties have seen considerable research attention, such as Gradient Vector Flow snake (GVFS) and the distance-transform based snake (DTS) of Cohen [4], or a balloon based pressure force [3] has been proposed which attracts active contours towards strong gradients, seeking to avoid noise and false gradients. However, in both cases there remain a number of parameters for the user to tune, parameters which vary from image to image.

In this paper, a novel deformable model for the accurate localization of object boundaries is introduced. Instead of minimizing the total energy of a snake, like most existing methods, our method performs coordinate descent, alternately maximizing the external energy within a specified region, then applying the prior constraints to force the boundary to satisfy required smoothness. The adaptivity of the method to sharp corners is satisfied by importance sampling the snake boundary points on the basis of curvature. Although our approach is parametric, users do not need to tune parameters for each image as the parameters are derived implicitly from image curvature and gradient. This proposed technique dramatically reduces computation time and improves the quality of the boundary solution compared to published snake methods irrespective of boundary geometry, image intensity and noise.

The rest of paper is organized as follows. Section 2 briefly addresses conventional snakes. Section 3 explains the proposed method, results of which and comparisons to other methods are given in Section 4.

2. BACKGROUND

A deformable model or snake is a spline

$$\mathbf{v}(s) = [x(s), y(s)], s \in [0, L] \tag{1}$$

where s is the arclength along the snake and L is the total length of snake. The “Energy” of a given snake is given by

$$E_{total} = \int_0^L \left[\underbrace{\alpha \left| \frac{\partial \mathbf{v}}{\mathrm{ds}} \right|^2}_{elasticity} + \underbrace{\beta \left| \frac{\partial^2 \mathbf{v}}{\mathrm{ds}^2} \right|^2}_{rigidity} + \gamma E_{ext}(\mathbf{v}) \right] ds \qquad (2)$$

where we see two terms, an internal energy function which behaves like a prior model, a smoothness constraint on the snake, and a second energy term E_{ext}, which is the external image force, generally assigned as the negative gradient of image intensity ($-\nabla I$). The desired solution is found by minimizing E_{total}, normally by discretizing the arclength s, representing the snake contour by some number of spline points.

3. PROPOSED METHOD

This proposed method involves the three iterative steps of optimal curve finding based on image gradients, snake point resampling, and snake estimation with prior constraints. Each of these steps is briefly described below.

3.1. Viterbi algorithm

We first seek a local perturbation to the current snake which gives the strongest fit to the image gradients. We are able to find the *optimum* local solution by formulating the problem as a Hidden Markov Model (HMM) and using a Viterbi search [6]. The discrete snake is defined in terms of $q-1$ straight line segments, parameterized by q discrete points, as illustrated in Fig 1(a). We search for image gradients normally to the snake curve at each of the q locations, such that each normal has p nodes distributed along its local length, also plotted in Fig 1(a). Each node represents a potential solution along that normal and, as a result, across all normals there are p^q potential solutions. Given measurements of E_{ext} for each of the p^q points, our goal is to find the best sequence of states which will maximize the probability function along the selected curve. The Viterbi algorithm computes the partial probability of each node in the trellis and identifies the most likely occurring path.

3.2. Curvature guided importance sampling

Due to image noise, the absence of prior constraints, the use of a local search, and the implicit first order Markov assumption, the optimal snake of the Viterbi method is typically not the desired snake. We will wish to assert constraints on the snake; in general, prior models for active contours choose first or second order constraints, which may cause problems for objects having high-curvature boundaries.

Therefore we propose a novel method to generate snake points using importance sampling of the local curvature (K) along the snake which will ensure more samples in high curvature regions, as illustrated in Fig 1(e). The density of samples is made proportional to the absolute value of curvature, but with a modified rejection approach to enforce upper and lower limits on the sample density, to avoid high-density singularities, and to avoid long under-sampled curves.

3.3. Statistical estimation

The prior constraints need to be accounted for and a tradeoff between the strength and significance of the image gradients versus the smoothness desired by the prior must be established. To directly incorporate prior shape models into the Viterbi approach is very difficult, even for relatively simple second-order constraints. For this reason that we have proposed a divided approach, allowing us to set up a prior-free Viterbi optimization, followed by a measurement — prior fusion step, here. Measurements of image gradient are taken at each resampled location,such that a measurement weight (essentially a measurement variance) is assigned to each sample based on the strength of the local gradient. The measurement — prior fusion proceeds as regular linear least squares [7]. where we assume a second-order prior, P, with measurements in M and the measurement weights (variances) in R.

$$\hat{Z} = (C^t R^{-1} C + P^{-1})^{-1} C^t R^{-1} M \qquad (3)$$

4. RESULTS AND CONCLUSIONS

We haved tested the proposed method on both synthetic and standard, published images (Face [8], disc [2], starfish [9], and thin u [5]). Experiments were performed on 2.6GHz AMD Athlon dual core machine.

For comparison purposes, published MATLAB code for the Gradient Vector Flow (GFV) snake, Traditional snake, Balloon Force (BF) snake and Distance Transformed Force (DTF) snake were acquired. For our method, the sampled points were constrained to be between 0.5 and 3.0 pixels apart. Parameters for the other four methods were set according to [5] and fixed for all test sets.

The results are shown in Fig. 3 and Fig. 4.In our proposed method, the snake parameters are guided by curvature and image gradients alone; as a result, the proposed method works effectively for all four images without adjusting any parameters. In contrast, the four comparative methods are sensitive to fixed parameters and no other method can effectively identify the necessary boundary for all test images. In particular, only our proposed method found the appropriate boundary for the starfish (B) and Face (D) image, which have complex boundary and also have an intensity that is highly nonuniform. The disc (C) poses challenges with a variety of edge strengths throughout the image and two of the methods (DTF snake and BF snake) did not converge for this image.

Fig 4 shows that the proposed method gives the best performance for both speed and MSE for *all* images across *all*

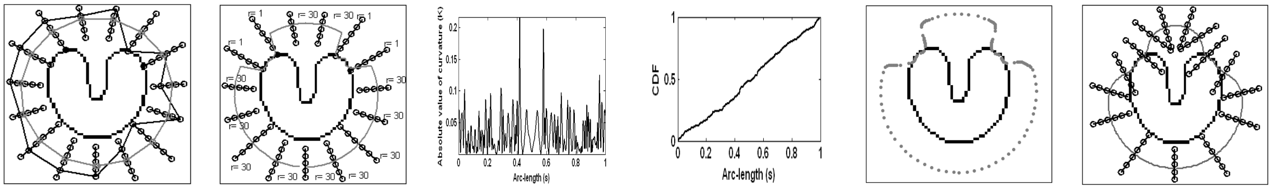

(a) (b) (c) (d) (e) (f)

Fig. 1. Illustration of one iteration of proposed method on a U-shaped object. (a) A circle (grey line) shows the initial positions of the snake, the jagged line shows a potential snake solution, and the small circles shows the nodes of Viterbi trellis. (b) The grey line shows the optimal snake after a Viterbi search. (c) Absolute value of curvature of the curve obtained using Viterbi search (X-axis arc length, Y-axis curvature). (d) CDF of absolute value of curvature on which importance sampling is carried out (e) Small circles are the particles generated using importance sampling on curvature of optimal Viterbi snake. (f) The grey line shows the estimated snake as the initial snake to start the next iteration.

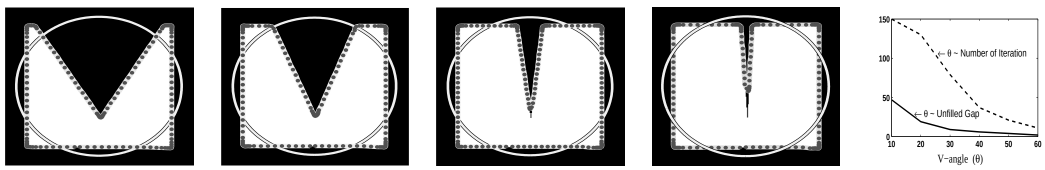

(a) (b) (c) (d) (e)

Fig. 2. Nature of convergence pattern of proposed method at various initial snake positions and geometry of object. White line and gray dots inside white line of Figure 2(a), (b), (c) and (d) are initial circular and final snake respectively. (e) shows the rate of convergence and remaining depth of hole ($Y - axis$) as a function of hole 'V-angle' (X-axis).

snake algorithms. Clearly, the proposed method is robust to noise relative to its peers Fig 3 (c), since the proposed method is the only method to successfully identify the diamond at all. GVFS, Traditional snake and Balloon force snake works well for image of Fig 3 (c), when the size of image is (64) and higher value of $\sigma = 5$ is used for denoising, but, in this paper the size of the u-shaped object is 512×512. On average, the proposed method is found to be 7 times faster with a 45 percent reduction in MSE.

In terms of sensitivity to concave shape, Fig. 2 shows four 'V' shape concave object and their successful convergence using the proposed method. In contrast, the balloon force (BF) snake requires that the initial snake be placed fully within the solution boundary [5]. Also, the Traditional snake requires an initial snake close to its solution to encourage speed of convergence and accuracy [5]. Further, slower convergence speed is a consistent concern for the GVF snake method.

In terms of parameter settings, a thorough experiment has been conducted to understand the effect of parameter estimation on the final solution for each of the five methods. That the final solution of our proposed method does not vary significantly for a wide range of parameters within the domain of our test case has been observed. However, for the other methods proper values of parameters are important for the snake to converge to the true solution. A test case showing how the convergence rate and difficulty in converging to very high curvature object is depicted in Fig. 2 (e), there we have plotted radial angle (an indicator of curvature) against convergence rate and remaining depth of gap for proposed snake.

We have proposed a novel deformable contour estimation method that is faster and more accurate than existing approaches. The method converges for a wide variety of difficult images, and is comparatively insensitive to initialization and parameter settings.

5. REFERENCES

[1] M. Kass, A. Witkin, and D. Terzopoulos, "Snakes: Active contour models," *IJCV*, vol. 1, no. 4, pp. 321–331, 1988.

[2] F.Y. Shih and Kai Zhang, "Locating object contours in complex background using improved snakes," *CVIU.*, vol. 105, no. 2, pp. 93–98, January 2007.

[3] L. D. Cohen, "On active contour models and balloons," *CVGIP*, vol. 53, no. 2, pp. 211–218, March 1991.

[4] Laurent D. Cohen and Isaac Cohen, "Finite-element methods for active contour models and balloons for 2-d and 3-d images," *IEEE Trans. on Pattern Anal. Mach. Intell.*, vol. 15, no. 11, pp. 1131–1147, 1993.

[5] C.Y. Xu and J.L. Prince, "Snakes, shapes, and gradient vector flow," *IEEE Trans. on Image Processing.*, vol. 7, no. 3, pp. 359–369, March 1998.

[6] A. J. Viterbi, "Error bounds for convolutional codes and an asymptotically optimum decoding algorithm," *IEEE Trans. on Information Theory*, vol. IT-13, pp. 260–269, 1967.

[7] Paul. Fieguth, "Statistical processing of multidimensional data," Course Notes for SD 770, 2007.

[8] Chieh-Chih Wang, "CMU VASC," 1998, http://vasc.ri.cmu.edu/idb/.

[9] Kahuna Bay, "Starfish- they are huge," Sept. 2007, http://kahunabay.wordpress.com/2007/09/07/starfish-they-are-huge/.

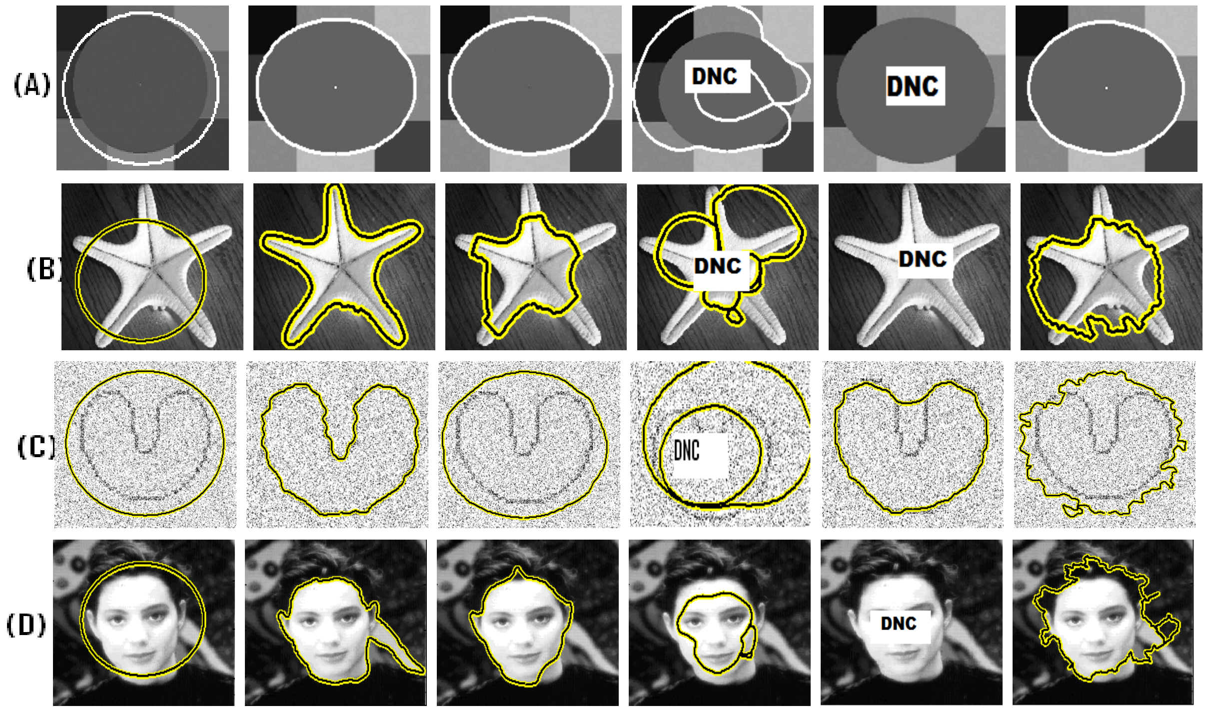

Initial Snake | Proposed Snake | Traditional Snake [1] | DTF Snake [4] | BF Snake [3] | GVF Snake [5]

Fig. 3. Column 1 shows initial circular snake. Column 2 shows snake generated using proposed method. Columns 3 to 6 show results using four other snake techniques [1, 3, 4, 5]. Black lines bounded by yellow lines are final contours. All four rows show images (A, B, C and D) obtained from [2, 5, 8, 9]. The proposed method is the only one that can properly identify the object boundary for each image. Some test cases did not converge (DNC).

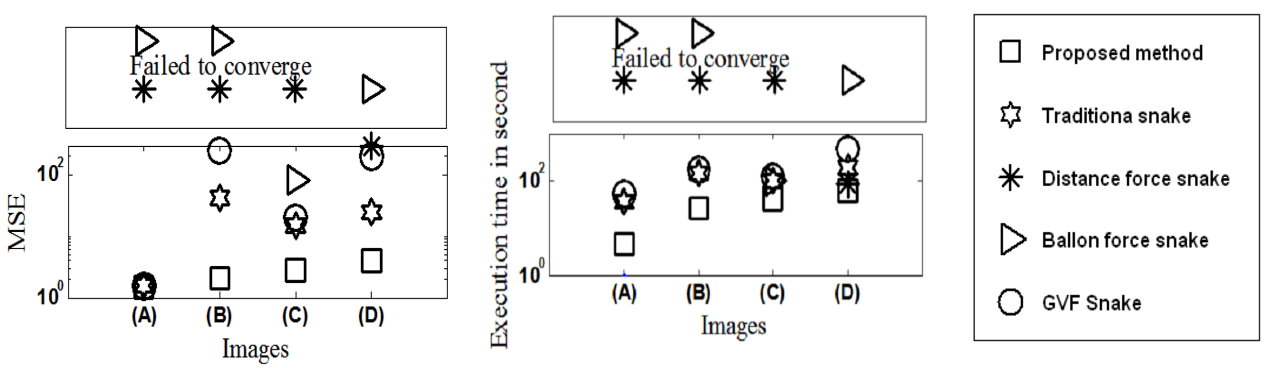

(a) (b) (c)

Fig. 4. Performance indices in terms of MSE and Execution time (sec). (a) MSE for each method across all four test images. (b) Execution time (in seconds) for each method across all four test images. (c) Symbols associated with each method.